Contribution from the ISSECC, CNR, 50132 Firenze, Italy, Dipartimento di Energetica dell'Università di Firenze, Firenze, Italy, and Dipartimento di Chimica dell'Università di Siena, Siena, Italy

Chemical and Electrochemical Oxidation of the Phosphoniodichalcogenoformate Complexes (triphos)RhCl(X_2CPEt_3) (triphos = $MeC(CH_2PPh_2)_3$; X = S, Se). Synthesis of Metal Dichalcogenocarbonates from O_2 and Phosphonium–Betaine-like Complexes. X-ray Structure of [(triphos)Rh($S_2CH(PEt_3)$)](BPh_4)$_2$

Claudio Bianchini,*† Andrea Meli,† Paolo Dapporto,‡ Anna Tofanari,‡ and Piero Zanello§

Received December 9, 1986

The phosphoniodichalcogenoformate complexes (triphos)RhCl(η^1-X_2CPEt_3) (X = S, **1**; Se, **2**) are chemically or electrochemically oxidized to [(triphos)RhCl(η^2-X_2CPEt_3)]$^{2+}$ (triphos = $MeC(CH_2PPh_2)_3$). These dications, which may add as many as two electrons to regenerate the starting compounds, react with EtOH, yielding octahedral phosphonium–betaine complexes of the formula [(triphos)RhCl($X_2CH(PEt_3)$)]$^+$. The five-coordinate derivatives [(triphos)Rh($X_2CH(PEt_3)$)]$^{2+}$ are obtained via chloride ligand elimination. Alternatively, the latter compounds can be prepared by the one-step reaction of **1** or **2** with $HOSO_2CF_3$ in the presence of $NaBPh_4$. Methylation of **1** by $MeOSO_2CF_3$ gives the analogous complex containing the novel $S_2CMe(PEt_3)^-$ ligand. The structure of [(triphos)Rh($S_2CH(PEt_3)$)](BPh_4)$_2$ has been determined by X-ray methods. Crystal data: monoclinic, space group $P2_1/n$, with a = 18.433 (6) Å, b = 27.384 (8) Å, c = 16.229 (6) Å, β = 92.25 (4)°, and Z = 4. The structure was refined to an R factor of 0.075 (R_w = 0.075) for 4906 unique reflections. The rhodium atom is coordinated by the three phosphorus atoms of triphos and by the two sulfur atoms of the $S_2CH(PEt_3)^-$ ligand in a distorted-square-pyramidal environment. The neutral or cationic dichalcogenocarbonate complexes (triphos)RhCl(S_2CO) and [(triphos)Rh(X_2CO)]$^+$ are obtained by reaction of O_2 with solutions of [(triphos)RhCl($S_2CH(PEt_3)$)]$^+$ and [(triphos)Rh($X_2CY(PEt_3)$)]$^{2+}$ (Y = H, Me), respectively. Pathways to the formation of the products are proposed and discussed.

Introduction

Despite the current interest in the coordination chemistry of X_2CPR_3 zwitterions (I; X = S,[1] Se;[2] R = alkyl), surprisingly little is still known about the reactivity of the resulting complexes. It

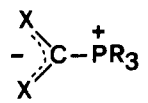

I

is now well-recognized that the carbon atom of the SS′-chelate triethylphosphoniodithioformate is an electrophilic center, susceptible to attack by various nucleophiles. As a result (i) addition products,[3] (ii) displacement of PEt_3 by the nucleophile,[1b] or (iii) products appropriate to substitution at the carbon atom[3b] are obtained.

By contrast, the reactions with electrophiles have been scarcely investigated. Such reactions, however, seem quite promising as suggested by the recently reported formation of the dichalcogenocarbonates (triphos)RhCl(X_2CO) from (triphos)RhCl(X_2CPEt_3) (X = S,[4] **1**; X = Se,[5] **2**) and O_2.

In this paper, we report on the reactions of **1** and **2** with chemical oxidants and electrophiles such as I_2, $NOBF_4$, Ag^+, H^+, and Me^+. In addition, we describe and discuss the formation of dichalcogenocarbonates by reaction of O_2 with phosphonium–betaine-like complexes (Schemes I and II).

Results

Synthesis and Characterization of the Complexes. Addition of I_2 to a THF solution of the phosphoniodithioformate complex **1** causes a rapid chromatic change from blue to red-orange, immediately followed by the precipitation of an orange powder. On further addition of I_2 the orange product dissolves while crystals of [(triphos)RhCl(S_2CPEt_3)](I_3)$_2$ (**3**) slowly form. Compound **3** is diamagnetic and poorly soluble in all common organic solvents but DMF. The $^{31}P\{^1H\}$ NMR spectrum in the latter solvent at 293 K exhibits an AB_2CX pattern with $\delta(P_A)$ = 23.88 (JP_A–Rh = 100.5 Hz, JP_A–P_B = 25.6 Hz, JP_A–P_C = 3.5 Hz), $\delta(P_B)$ = 5.03 ($J(P_B$–Rh) = 97.0 Hz, $J(P_B$–$P_C)$ = 10.4 Hz), and $\delta(P_C)$ = 47.64 ($J(P_C$–Rh) = 5.2 Hz). The IR spectrum contains a medium-intensity band at 1030 cm^{-1} due to the C–CH_3 rocking of the PEt_3 group.[4] No band attributable to ν(C=S) can be found, although such a vibration is present in the spectrum of the starting compound **1**. This fact is probably due to the increased ability of Rh(III) versus that of Rh(I) to withdraw electron density from the 1,1-dithio ligand, which, in addition, uses both its sulfur atoms to link the metal. On the basis of all these data, **3** is assigned the structural formulation shown in Scheme I. The orange powder that first forms during the reaction is formulated as [(triphos)-RhCl(S_2CPEt_3)]I_2 (**4**). In fact, compounds **3** and **4** exhibit identical ^{31}P NMR spectra. In addition, **4** is quantitatively converted to **3** by treatment with I_2.

The bonding model of the zwitterionic ligand changes from η^1 to η^2 on going from **1** to **3** as the natural consequence of the increased oxidation state of the metal (from +1 to +3). Interestingly, the process is reversible; the reduction of **3** and **4** as well with $LiHBEt_3$ in benzene quantitatively restores the starting compound **1**.

Compound **3** is air-stable both in the solid state and in nonalcoholic solvents. In contrast, when the compound is dissolved in a 4:1 DMF/EtOH mixture, a slow reaction takes place as evidenced by the $^{31}P\{^1H\}$ NMR spectrum of the red-orange complex [(triphos)RhCl($S_2CH(PEt_3)$)]I_3 (**5**), which can be obtained on further addition of ethanol. In fact, although the NMR pattern remains of the AB_2CX type, different chemical shifts are observed. These are $\delta(P_A)$ = 13.37 ($J(P_A$–Rh) = 98.0 Hz, $J(P_A$–$P_B)$ = 23.6 Hz, $J(P_A$–$P_C)$ = 3.5 Hz), $\delta(P_B)$ = 5.31 ($J(P_B$–Rh) = 97.8 Hz, $J(P_B$–$P_C)$ = 11.7 Hz), and $\delta(P_C)$ = 46.10 ($J(P_C$–Rh) = 5.8 Hz). Compound **5** is air-stable in the solid state but slowly decomposes in solution unless air is excluded. The presence of the unusual phosphonium–betaine ligand $S_2CH(PEt_3)^-$ is evidenced by its ^1H NMR spectrum (DMF, 293 K) containing a multiplet at δ 5.20 (1 H), which can be assigned to the hydrogen atom of $S_2CH(PEt_3)^-$.[6]

† ISSECC, CNR.
‡ University of Firenze.
§ University of Siena.

(1) (a) Bianchini, C.; Ghilardi, C. A.; Meli, A.; Midollini, S.; Orlandini, A. *Organometallics* **1982**, *1*, 1058. (b) Bianchini, C.; Innocenti, P.; Meli, A.; Orlandini, A.; Scapacci, G. *J. Organomet. Chem.* **1982**, *233*, 233. (c) Bianchini, C.; Ghilardi, C. A.; Meli, A.; Orlandini, A.; Scapacci, G. *J. Chem. Soc., Dalton Trans.* **1983**, 1969. (d) Bianchini, C.; Ghilardi, C. A.; Meli, A.; Orlandini, A. *Inorg. Chem.* **1983**, *22*, 2188. (e) Baird, D. M.; Fanwick, P. E.; Barwick, T. *Inorg. Chem.* **1985**, *24*, 3753. (f) Miguel, D.; Riera, V.; Miguel, J. A.; Solāns, X.; Font-Altaba, M. *J. Chem. Soc., Chem. Commun.* **1987**, 472.
(2) Otto, H.; Ebner, M.; Werner, H. *J. Organomet. Chem.* **1986**, *311*, 63 and references therein.
(3) (a) Bianchini, C.; Mealli, C.; Meli, A.; Scapacci, G. *Organometallics* **1983**, *2*, 141. (b) Bianchini, C.; Meli, A.; Orlandini, A. *Inorg. Chem.* **1982**, *21*, 4166.
(4) Bianchini, C.; Mealli, C.; Meli, A.; Sabat, M. *J. Chem. Soc., Chem. Commun.* **1985**, 1024.
(5) Bianchini, C.; Mealli, C.; Meli, A.; Sabat, M. *J. Am. Chem. Soc.* **1985**, *107*, 5317.

0020-1669/87/1326-3677$01.50/0

Scheme I

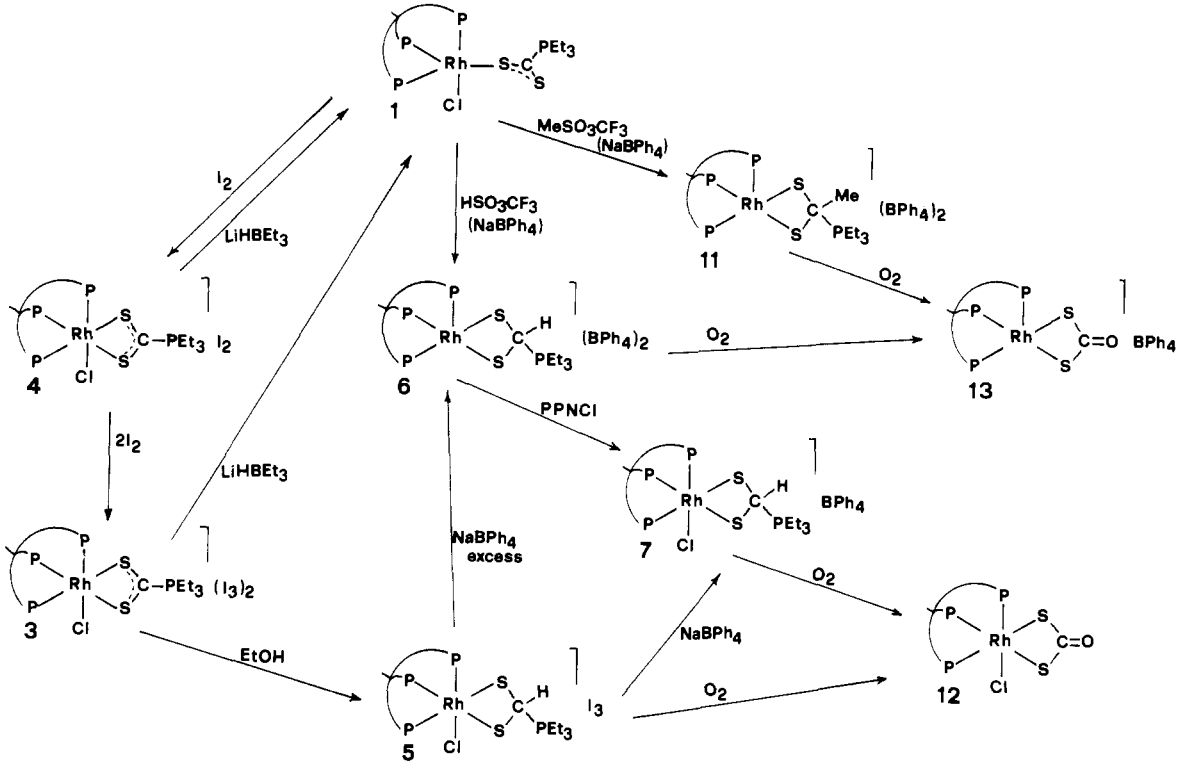

Scheme II

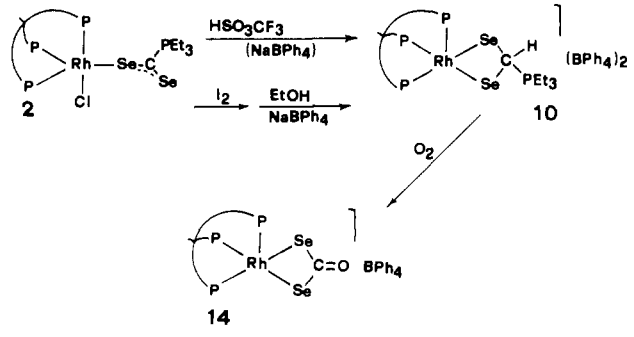

Reaction of **5** in CH_2Cl_2–EtOH with a large excess of $NaBPh_4$ gives red crystals of $[(triphos)Rh(S_2CH(PEt_3))](BPh_4)_2$ (**6**). Compound **6**, analogously to **5**, is stable in the solid state and in deoxygenated solvents. The $^{31}P\{^1H\}$ NMR spectrum (DMF, 293 K) exhibits an AB_3X system with resonances at 35.42 ppm ($\delta(P_B)$, triphos, $J(P_B\text{–}Rh)$ = 96.6 Hz, $J(P_B\text{–}P_A)$ = 11.9 Hz), and 43.65 ppm ($\delta(P_A)$, PEt_3, $J(P_A\text{–}Rh)$ = 3.7 Hz) (relative intensities 3:1). No variation of the pattern was observed in the temperature range 213–313 K. The equivalence of the three phosphorus atoms of triphos, as revealed by the ^{31}P NMR spectrum, occurs whenever the metal is five-coordinate and is due to the rapid intramolecular exchange of the phosphorus atoms.[4] The integrity of the $S_2CH(PEt_3)^-$ ligand in **6** is confirmed both by the ^1H NMR spectrum (DMF, 293 K) containing the resonance of the phosphonium–betaine proton at δ 5.20 and by the IR spectrum exhibiting the typical absorption of the PEt_3 group. Furthermore, the addition of Cl^- anions from (PPN)Cl (PPN = bis(triphenylphosphine)-nitrogen(1+)) to a solution of **6** gives $[(triphos)RhCl(S_2CH(PEt_3))]BPh_4$ (**7**), obtainable also by metathetical reaction of **5** with $NaBPh_4$.

The crystal and molecular structure of **6** consists of monomeric complex cations $[(triphos)Rh(S_2CH(PEt_3))]^{2+}$ and BPh_4^- anions. Figure 1 shows a perspective view of the complex cation whose selected bond distances and angles are reported in Table II. As

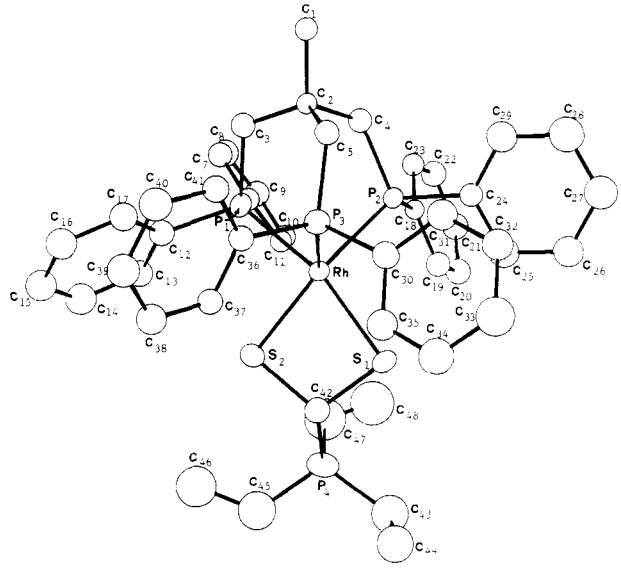

Figure 1. ORTEP drawing and labeling scheme for $[(triphos)Rh(S_2CH(PEt_3))](BPh_4)_2$ (**6**).

expected from the chemical–physical characterization of the complex, the metal is coordinated by the three phosphorus atoms of triphos and by the two sulfur atoms of the $S_2CH(PEt_3)^-$ ligand in a distorted-square-pyramidal environment. Such a distortion is exhibited by all of the other complexes containing phosphonium–betaine ligands, namely $[(etriphos)Co(S_2CH(PEt_3))](BPh_4)_2$[6a] and $[Ru(S_2CH(PMe_2Ph))(PMe_2Ph)_3]PF_6$,[7] and is mainly due to the short bite of the 1,1-dithio ligand (the S(1)–Rh–S(2) angle is 75.1 (3)°). The rhodium atom lies away from the least-squares basal plane (0.38 Å) toward the P(3) apical atom. The Rh–P(3) distance, 2.226 (6) Å, is significantly shorter than the two Rh–P basal distances, 2.313 (7) and 2.311 (6) Å, as expected for C_{4v} low-spin d^6 metal complexes.[8] The angles in-

(6) (a) Bianchini, C.; Meli, A.; Orlandini, A. *Inorg. Chem.* **1982**, *21*, 4161. (b) Werner, H.; Bertleff, W. *Chem. Ber.* **1980**, *113*, 267.

(7) Ashworth, T. V.; Singleton, E.; Laing, M. *J. Chem. Soc., Chem. Commun.* **1976**, 875.

(8) Rossi, A. R.; Hoffmann, R. *Inorg. Chem.* **1975**, *14*, 365.

Table I. Crystallographic Parameters for **6**

formula	$C_{96}H_{95}B_2P_4RhS_2$
mol wt	1651.24
cryst size, mm	0.50 × 0.25 × 0.25
space group	$P2_1/n$
a, Å	18.433 (6)
b, Å	27.384 (8)
c, Å	16.229 (6)
β, deg	92.25 (4)
V, Å^3	8185.6
Z	4
d_{calcd}, g cm^{-3}	1.267
μ(Mo Kα), cm^{-1}	3.30
radiation	graphite-monochromated Mo Kα (λ = 0.710 69 Å)
scan type	$\omega/2\theta$
2θ range, deg	6–50
scan width, deg	0.8 + 0.3 tan ω
scan speed, deg s^{-1}	0.07
total data	12 868
unique data, $I \geq 3\sigma(I)$	4906
no. of params	288
R	0.075
R_w	0.075
w	$1/\sigma^2(F_o)$

Table II. Selected Bond Distances (Å) and Angles (deg)

Rh–P(1)	2.313 (7)	P(2)–C(24)	1.82 (2)
Rh–P(2)	2.311 (6)	P(3)–C(5)	1.83 (2)
Rh–P(3)	2.226 (6)	P(3)–C(30)	1.82 (2)
Rh–S(1)	2.352 (7)	P(3)–C(36)	1.82 (2)
Rh–S(2)	2.300 (7)	P(4)–C(42)	1.80 (2)
P(1)–C(3)	1.84 (2)	P(4)–C(43)	1.78 (3)
P(1)–C(6)	1.81 (2)	P(4)–C(45)	1.76 (3)
P(1)–C(12)	1.82 (2)	P(4)–C(47)	1.94 (4)
P(2)–C(4)	1.83 (2)	S(1)–C(42)	1.79 (2)
P(2)–C(18)	1.80 (2)	S(2)–C(42)	1.82 (2)
P(1)–Rh–P(2)	90.1 (2)	C(4)–P(2)–C(24)	108.2 (9)
P(1)–Rh–P(3)	89.4 (2)	C(18)–P(2)–C(24)	101.4 (8)
P(1)–Rh–S(1)	161.2 (3)	Rh–P(3)–C(5)	113.3 (8)
P(1)–Rh–S(2)	89.8 (3)	Rh–P(3)–C(30)	114.0 (5)
P(2)–Rh–P(3)	85.9 (2)	Rh–P(3)–C(36)	110.9 (6)
P(2)–Rh–S(1)	99.2 (2)	C(5)–P(3)–C(30)	107.4 (9)
P(2)–Rh–S(2)	156.6 (2)	C(5)–P(3)–C(36)	108.0 (9)
P(3)–Rh–S(1)	107.4 (3)	C(30)–P(3)–C(36)	102.6 (8)
P(3)–Rh–S(2)	117.4 (3)	C(42)–P(4)–C(43)	107.9 (15)
S(1)–Rh–S(2)	75.1 (3)	C(42)–P(4)–C(45)	111.0 (15)
Rh–P(1)–C(3)	113.6 (8)	C(42)–P(4)–C(47)	110.9 (16)
Rh–P(1)–C(6)	109.5 (5)	C(43)–P(4)–C(45)	107.6 (18)
Rh–P(1)–C(12)	115.2 (6)	C(43)–P(4)–C(47)	115.8 (17)
C(3)–P(1)–C(6)	108.7 (9)	C(45)–P(4)–C(47)	103.6 (19)
C(3)–P(1)–C(12)	105.4 (9)	Rh–S(1)–C(42)	90.0 (8)
C(6)–P(1)–C(12)	103.7 (7)	Rh–S(2)–C(42)	90.9 (8)
Rh–P(2)–C(4)	110.7 (8)	S(1)–C(42)–P(4)	114.6 (13)
Rh–P(2)–C(18)	111.6 (5)	S(2)–C(42)–P(4)	112.5 (14)
Rh–P(2)–C(24)	118.9 (6)	S(1)–C(42)–S(2)	103.4 (13)
C(4)–P(2)–C(18)	104.9 (9)		

volving the $>CS_2$ fragment, S(1)–C(42)–S(2) = 103.4 (13)°, S(1)–C(42)–P(4) = 114.6 (13)°, and S(2)–C(42)–P(4) = 103.4 (13)°, are typical of an sp^3 carbon atom, and therefore we conclude that a hydrogen atom is linked to C(42), which is consistent with the ^{1}H NMR results. The two S–C(42) bond distances, 1.79 (2) and 1.82 (2) Å, and the P(4)–C(42) distance of 1.80 (2) Å, being indicative of single bonds, confirm the sp^3 hybridization of this carbon atom. The four-membered RhS_2C ring is essentially planar, the deviations from the least-squares plane of the four atoms being below 0.06 Å.

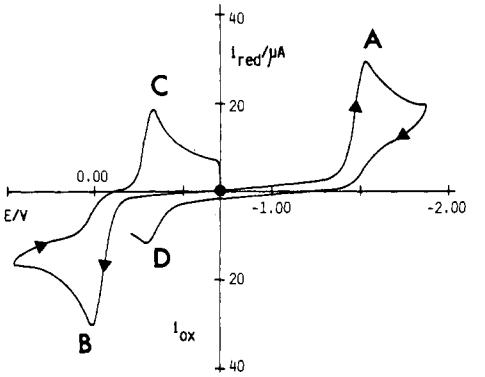

Figure 2. Cyclic voltammogram recorded at a platinum electrode on a MeCN solution containing **1** (1.75×10^{-3} mol dm^{-3}) and $(NEt_4)ClO_4$ (0.1 mol dm^{-3}) (scan rate 0.2 V s^{-1}). The black circle (●) indicates the starting potential for cyclic scans.

The compounds $[(triphos)RhCl(S_2CH(PEt_3))]BF_4$ (**8**) and $[(triphos)Rh(S_2CH(PEt_3))](BF_4)_2$ (**9**) are synthesized by reacting **1** with other chemical oxidants such as $NOBF_4$ or $AgBF_4$. It is obvious that when the chloride ligand is not removed from the metal, only **8** is obtained. In any case, however, the presence of EtOH is mandatory to get the compounds.

The reactivity of the selenium derivative **2** toward oxidizing agents is identical with that of **1**. As a matter of fact, the oxidation of **2** by I_2, $NOBF_4$, or $AgBF_4$ followed by addition of $NaBPh_4$ in ethanol gives $[(triphos)Rh(Se_2CH(PEt_3))](BPh_4)_2$ (**10**), which is the first metal complex containing a $Se_2CH(PR_3)^-$ ligand. The brown complex **10** has been assigned the structure of **6** since the two compounds share almost identical physical–chemical properties. As an example, the $^{31}P\{^1H\}$ NMR spectrum (DMF, 293 K) exhibits an AB_3X pattern with $\delta(P_B)$ = 33.75 ($J(P_B–Rh)$ = 97.6 Hz, $J(P_B–P_A)$ = 85.0 Hz), and $\delta(P_A)$ = 43.12 ($J(P_A–Rh)$ not detectable) (Scheme II).

Compounds **1** and **2** dissolved in THF react with stoichiometric amounts of H^+ from $HOSO_2CF_3$ or HBF_4 in the presence of $NaBPh_4$ to yield **6** and **10**, respectively.

Under the same conditions, methylation of **1** by $MeOSO_2CF_3$ gives the complex $[(triphos)Rh(S_2CMe(PEt_3))](BPh_4)_2$ (**11**), which contains the novel $S_2CMe(PEt_3)^-$ ligand.

Compounds **6**, **10**, and **11** exhibit close physical–chemical properties. The $^{31}P\{^1H\}$ NMR spectrum (DMF, 293 K) of **11** is of the AB_3X type with chemical shifts and coupling constants essentially concident with those of **6** and **10** ($\delta(P_A)$ = 43.32, PEt_3, $J(P_A–P_B)$ = 11.8 Hz, $J(P_A–Rh)$ = 3.8 Hz; $\delta(P_B)$ = 35.29, triphos, $J(P_B–Rh)$ = 96.5 Hz). Unfortunately, the presence of a methyl substituent on the sp^3 carbon atom of the 1,1-dithiolate ligand cannot be detected by ^{1}H NMR spectroscopy because the region is masked by the resonances of the methyl groups of PEt_3. However, in view of all of the other data, compound **11** is assigned the primary structure of **6**.

Electrochemistry. The redox properties of **1** have been primarily tested by cyclic voltammetry. Figure 2 shows the relevant responses in acetonitrile solvent. Both the cathodic process occurring at peak A and the anodic process occurring at peak B display an associated response in the reverse scan. However, while peak D,

Table III. Positional Parameters (×10^4), Anisotropic Temperature Factors (×10^3),[a] and Estimated Standard Deviations

atom	x/a	y/b	z/c	U_{11}	U_{22}	U_{33}	U_{12}	U_{13}	U_{23}
Rh	196 (1)	2475 (1)	2072 (1)	32 (1)	33 (1)	40 (1)	4 (1)	2 (1)	0 (1)
P(1)	500 (2)	2167 (1)	808 (2)	39 (2)	46 (2)	41 (2)	6 (2)	4 (2)	4 (2)
P(2)	−312 (2)	1732 (1)	2414 (2)	34 (2)	38 (2)	41 (2)	2 (2)	7 (2)	−1 (2)
P(3)	1227 (2)	2176 (1)	2626 (2)	34 (2)	40 (2)	48 (3)	0 (2)	−4 (2)	2 (2)
P(4)	−890 (2)	3902 (1)	2284 (3)	56 (3)	50 (3)	107 (4)	8 (2)	4 (3)	−2 (3)
S(1)	−327 (2)	2967 (1)	3073 (2)	94 (3)	47 (2)	56 (3)	15 (2)	25 (2)	−2 (2)
S(2)	223 (2)	3254 (1)	1535 (3)	71 (3)	41 (2)	75 (3)	9 (2)	23 (2)	11 (2)

[a] Anisotropic thermal factors are of the form $\exp[-2\pi^2(U_{11}h^2a^{*2} + U_{22}k^2\beta^{*2} + U_{33}l^2c^{*2} + 2U_{12}hka^*b^* + ...)]$.

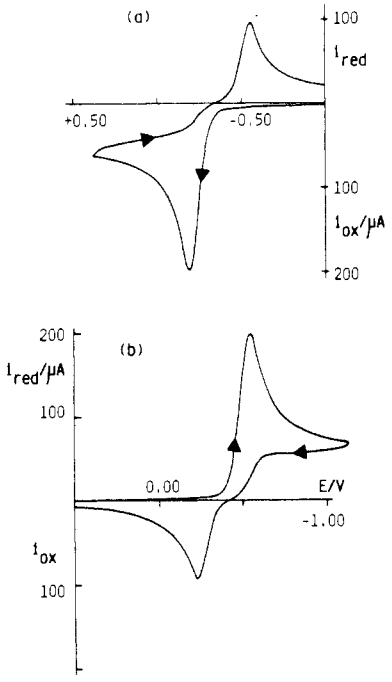

Figure 3. Cyclic voltammograms recorded at a platinum electrode on a MeCN solution containing **1** (1.6×10^{-1} mmol) and $(NEt_4)ClO_4$ (0.1 mol dm^{-3}). Under the following experimental conditions: (a) initial scan; (b) scan after the two-electron oxidation at +0.2 V.

which is notably far from the parent peak A, is most likely due to fragmentation products of the starting framework, peak C can be directly associated with the reduction of the species primarily electrogenerated at peak B. Controlled-potential coulometric tests performed in correspondence with the anodic process (E_w = +0.3 V) led to the consumption of 2 mol of electrons/mol of **1**. Solution samples systematically withdrawn at different stages of the electrolysis were revealed to be constantly ESR silent. In the meantime, the blue solution turned red-orange. Figure 3b shows the cyclic voltammogram recorded after the bulk electrolysis. The two-electron oxidation gives rise to a voltammogram complementary to that prior to electrolysis; i.e., the initial anodic current is now cathodic and vice versa. In addition, the successive cathodic electrolysis at −0.5 V still consumes 2 mol of electrons/mol of starting unit, causing the solution to assume the initial blue color while the resulting cyclic voltammogram is identical with that shown in Figure 2. Noticeably, the cyclic voltammetric response of **3** is identical with that reported in Figure 3b. These results incontrovertibly support the chemical reversibility of the two-electron oxidative process $\mathbf{1} \rightleftharpoons \mathbf{3} + 2e^-$. On this basis it is interesting to analyze the features of the cyclic voltammetric response B/C in Figure 2. Tests at scan rates v gradually varying from 0.02 to 50 V s^{-1} provide the following diagnostic parameters:[9] the current function $i_{p(B)}v^{-1/2}$ slightly decreases (<20%); the $i_{p(C)}/i_{p(B)}$ ratio is constantly equal to 0.95; the difference ΔE_p gradually increases from 310 to 540 mV;[10] $E_{p(B)} - E_{p/2}$ is equal to 70 mV; $E_{p(B)}$ anodically shifts 35 mV per 10-fold increase in scan rate.

In the commonly accepted assumption that multielectron processes proceed through one-electron steps, it must be taken into account that, for a two-electron transfer, the appearance of a single response arises either when the standard electrode potentials for each one-electron transfer are coincident ($E^\circ_1 = E^\circ_2$) or when the second step is easier than the first one ($E^\circ_2 > E^\circ_1$). In both cases, if the overall process is electrochemically reversible, the following results are expected:[11] $i_{pc}/i_{pa} = 1$, $i_{pa}v^{-1/2}$ = constant;

(9) Brown, E. R.; Large, R. F. In *Techniques of Chemistry*; A. Weissberger, A., Rossiter, B. W., Eds.; Wiley-Interscience: New York, 1971; Part IIA, Chapter VI.
(10) Under the same experimental conditions, the one-electron oxidation of ferrocene displays a ΔE_p value of 70 mV, thereby disregarding the occurrence of large uncompensated solution resistances.
(11) Polcyn, D. S.; Shain, I. *Anal. Chem.* **1966**, *38*, 370.

Table VI. Peak Potential Values (in V versus Fc^+/Fc) for the Redox Changes of **1** in Different Solvents at the Scan Rate of 0.2 V s^{-1}

	anodic process		cathodic process
solvent	E_{pa}	E_{pc}	E_{pc}
MeCN	−0.32	−0.69	−1.91
CH_2Cl_2	−0.28	−0.75	−1.99

$E_{pa} - E_{p/2}$ near 20 mV, ΔE_p near 30 mV.[12] Hence, it is evident that, in the present case, the chemically reversible anodic process involves a two-electron step with marked departure from the electrochemical reversibility. Essentially, the same behavior holds in CH_2Cl_2 solvent. In effect, two alternative causes may be responsible for the slow electron-transfer rate: (a) an intrinsic feature of the interaction between the reactant molecule and the electrode surface; (b) a drastic conformational reorganization occurring in the framework of the starting molecule in consequence of the removal of two electrons. Both the solvent independence of the responses and the chemical evidence reported in the previous section strongly support the occurrence of the structural rearrangement $Rh(\eta^1\text{-}S_2CPEt_3) \rightarrow Rh(\eta^2\text{-}S_2CPEt_3)$. A number of stereochemical changes concomitant with charge transfers have been recently observed.[13] In particular, Geiger and Tulyathan[14] have examined the structure/redox relationships for reaction 1.

$$\underset{\text{bicapped tetrahedral}}{Os_6(CO)_{18}} \underset{-2e^-}{\overset{+2e^-}{\rightleftharpoons}} \underset{\text{octahedral}}{[Os_6(CO)_{18}]^{\bullet 2-}} \qquad (1)$$

They argued that the two-electron reduction proceeds through two sequential one-electron transfers: the second step is that thermodynamically favored whereas the electron-transfer rate is determined by the first one. The low rate of this step is due to the enhancement of the energy barrier of the heterogeneous charge transfer caused in good part by the structural reorganization of the cluster framework (see (1)). Notice, however, that reorientations of solvent dipoles following the appearance of charge in the molecule cannot be neglected. Indeed, the anodic process described here is quite reminiscent of Geiger's model but diagnostic parameters (particularly $i_{pc}/i_{pa} < 1$) suggest that the slow step is confined to the removal of the second electron.

As far as the cathodic process occurring at peak A is concerned, cyclic voltammograms at different scan rates indicated its electrochemical irreversibility, probably because of fast chemical reactions coupled to the charge transfer. In fact, even at 50 V s^{-1}, a directly associated reoxidation process could not be detected. Controlled-potential coulometry performed at −1.7 V showed that two mol of electrons/mol of **1** was consumed. The totally decomplexing character of this redox change was pointed out by the fact that, after the exhaustive electrolysis, a series of minor irreversible responses were recorded in the relevant cyclic voltammogram (i.e. a further cathodic response at −1.95 V and two anodic responses at −0.30 (in correspondence of peak D) and −0.05 V, respectively) together with a prominent irreversible process at +0.90 V. The latter is attributed to the oxidation of free triphos released during the reduction. In addition, controlled-potential electrolyses performed in correspondence with each of these processes did not restore the starting derivative.

Table VI summarizes the redox potentials of **1** in different solvents relative to the ferrocene/ferrocenium couple used as internal reference.[15]

Discussion

Phosphonium–betaine ligands of the type $S_2CH(PEt_3)^-$ may form by two different mechanisms. One involves nucleophilic

(12) Significant differences between the two mechanisms are observed in current parameters rather than in potential parameters.
(13) (a) Evans, D. H.; O'Connel, K. M. In *Electroanalytical Chemistry*; Bard, A. J., Ed.; Marcel Dekker: New York, 1986; Vol. 14, p 113. (b) Osella, D.; Gobetto, R.; Montangero, P.; Zanello, P.; Cinquantini, A. *Organometallics* **1986**, *5*, 1247. (c) Bianchini, C.; Mealli, C.; Meli, A.; Sabat, M.; Zanello, P. *J. Am. Chem. Soc.* **1987**, *109*, 185.
(14) Tulyathan, B.; Geiger, W. E. *J. Am. Chem. Soc.* **1985**, *107*, 5960.
(15) Under the present experimental conditions, the ferrocene/ferrocenium couple is located at +0.36 V in MeCN and at +0.48 V in CH_2Cl_2.

attack by a tertiary phosphine at an η^2-coordinated dithioformate ligand (eq 2).[16] Alternatively, the nucleophile and the electrophilic

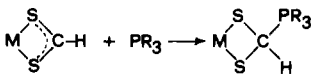
(2)

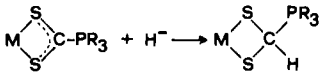
(3)

site are H^- and the central carbon atom of a zwitterionic S_2CPR_3 ligand, respectively (eq 3).[3a,6] Both reaction paths may occur either intra- or intermolecularly.

The reactions leading to **5**, **6**, and **10** are such that only mechanism 3 is accessible, the H^- species being most likely provided by EtOH. In fact, recall that the presence of alcohol in the reaction mixture is mandatory to get the $X_2CPEt_3 \rightarrow X_2CH(PEt_3)^-$ conversion (X = S, Se). How the latter process may go through it is hard to assess in the absence of detectable intermediates as well as of kinetic measurements. There are two possible pathways: (i) direct abstraction of an hydridic hydrogen atom from EtOH by the X_2CPEt_3 carbon atom; (ii) preliminary formation of a rhodium hydride complex followed by H^- transfer to the zwitterionic ligand. In both cases, the X_2CPEt_3 carbon is expected to have electrophilic nature. In effect, this carbon, which does not possess any particular character in the free zwitterions, becomes undoubtedly electrophilic in metal complexes.[1b,3,6a] Indirect support for the intramolecular hydride migration as a possible mechanistic step for the formation of **5**, **6**, and **10** is provided by the reactions of **1** and **2** with H^+ and Me^+. In fact, only 1 equiv of E^+ (E = H, Me) is responsible for both metal oxidation and formation of the reaction products. Accordingly, the most palatable mechanistic interpretation is to think of the preliminary attack by the electrophile at the occupied frontier σ orbital that d^8 ML_5 systems such as complexes **1** and **2** may arrange upon slight displacement of the coordinated chalcogen atom in the equatorial plane of the trigonal bipyramid (eq 4).[17]

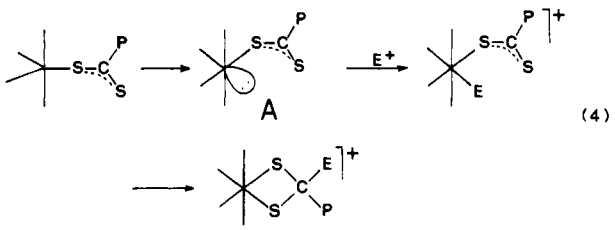
(4)

As a consequence, the oxidation state of the metal is raised by two units and the geometry becomes octahedral. The subsequent migration of the E group to the carbon of X_2CPEt_3 may be forced by the uncoordinated X atom of the latter ligand, which ultimately reaches the more stable chelate configuration. In any case, complexes containing $[(triphos)RhCl(X_2CH(PEt_3))]^+$ cations form, which upon elimination of Cl^- by $NaBPh_4$ transform into $[(triphos)Rh(X_2CH(PEt_3))]^{2+}$.

Also, mechanism 4 has the additional merit of providing a plain explanation for the oxidations of **1** and **2** by I_2, $NOBF_4$, or $AgBF_4$. In fact, after being attacked by electrophiles, the metal lone pair shown in intermediate A may be thought of as being either electrochemically or chemically removed. As a result, the uncoordinated chalcogen atom becomes a new potential donor for rhodium, which now is in oxidation state +3.

When solutions of **5**, **6**, **7**, **10**, and **11** are exposed to atmospheric oxygen or reacted with pure dioxygen, dithio- (**12** and **13**) or diselenocarbonates (**14**) form (Schemes I and II).[4,5] The formation of dithiocarbonates from O_2 and metal complexes containing 1,1-dithiolate ligands of the type $S_2CX(Y)$ (X, Y = H, OEt; H, SMe; H, PEt_3; SMe, PEt_3) is a rather general process.[3b,18] Detailed studies on the mechanism for these reactions have not been performed. However, it appears reasonable, from the nature of both the reagents and the products, that, at a certain stage of the reactions, some electron density accumulates on the central carbon atom of the 1,1-dithio ligand. A palatable way by which electron density may become available at this carbon atom is to think of *a sort of reductive elimination* of XY. As a result, an electron-rich carbenoid carbon forms, which is appropriate for electrophilic attack by dioxygen (eq 5). Indeed, most of the X

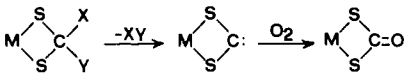
(5)

and Y substituents may give rise to excellent leaving groups such as EtOH, MeSH, and $HPEt_3^+$ and, in effect, the last two have been detected as byproducts of the decomposition of (triphos)$Co(S_2CH(SMe))$, $[(triphos)Co(S_2CH(PEt_3))]^+$,[18] and (triphos)$Ni(S_2CH(SMe))$.[3a]

Although quite unusual in coordination chemistry, 1,3-dithiolium carbenes are well-recognized as intermediates in the reactions of CS_2 with activated alkynes (eq 6).[19] Such 1,3-dithiolium carbenes may be trapped by alcohols to give alkoxydithioles through a process that, in practice, corresponds to the reverse of that shown in (5).

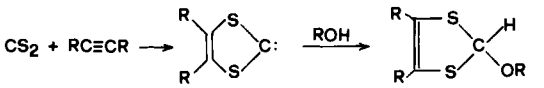
(6)

Experimental Section

All the reactions and manipulations were routinely performed under a nitrogen atmosphere unless otherwise stated. All materials and solvents were of reagent-grade quality and were used without further purification. The complexes (triphos)$RhCl(S_2CPEt_3)$[4] and (triphos)$RhCl(Se_2CPEt_3)$[5] were prepared by published procedures. The solid complexes were collected on a sintered-glass frit, appropriately washed, and finally dried in a stream of nitrogen. IR spectra were recorded on a Perkin-Elmer 283 spectrophotometer as Nujol mulls between KBr plates. $^{31}P\{^1H\}$ and ^1H NMR spectra were recorded with a Varian CFT 20 spectrometer. Peak positions are relative to tetramethylsilane and phosphoric acid with downfield values reported as positive. The electrochemical apparatus as well as the relevant materials have been described elsewhere.[13c] Unless otherwise specified, potential values, measured at 20 ± 0.1 °C, refer to a saturated calomel electrode.

Reaction of 1 with I_2. A THF (10 mL) solution of I_2 (0.51 g, 2 mmol) was added dropwise to a rapidly stirred solution of **1** (0.48 g, 0.5 mmol) in THF (70 mL). An immediate reaction occurred; the starting blue solution became red-orange, and $[(triphos)RhCl(S_2CPEt_3)]I_2$ (**4**) precipitated as an orange powder. Further addition of I_2 caused the powder to dissolve. Red-orange crystals of $[(triphos)RhCl(S_2CPEt_3)](I_3)_2$ (**3**) precipitated on standing. They were filtered off and washed with a 1:1 mixture of THF–*n*-pentane; yield 80%. Compound **4** could be isolated in 75% yield by reacting **1** with an equivalent amount of I_2. By treatment of a THF suspension of **4** with a 3-fold excess of I_2, **3** could be obtained in quantitative yield. Anal. Calcd for $C_{48}H_{54}Cl_7P_4RhS_2$ (**3**): C, 33.54; H, 3.17; Rh, 5.99. Found: C, 33.48; H, 3.13; Rh, 5.91. Anal. Calcd for $C_{48}H_{54}CI_2P_4RhS_2$ (**4**): C, 47.60; H, 4.49; Rh, 8.50. Found: C, 47.52; H, 4.43; Rh, 8.65.

Reaction of 3 or 4 with $LiHBEt_3$. Addition of $LiHBEt_3$ (1 M in THF, 0.5 mL) to a suspension of **3** or **4** (0.2 mmol) in benzene (60 mL) caused the solid to dissolve to give a deep blue solution. Blue crystals of **1** quantitatively precipitated on standing.

Reaction of 3 with EtOH. A solution of **3** (0.34 g, 0.2 mmol) in a 4:1 mixture of DMF–EtOH (10 mL) was stirred for 1 h. Further addition of ethanol (60 mL) led to the precipitation of red-orange crystals of $[(triphos)RhCl(S_2CH(PEt_3))]I_3$ (**5**), which were filtered off and washed with ethanol and petroleum ether; yield 70%. Anal. Calcd for

(16) (a) Ashworth, T. V.; de Waal, D. J. A.; Singleton, E. *J. Chem. Soc., Chem. Commun.* **1981**, 78. (b) Einstein, F. W.; Enwall, E.; Flitcraft, N.; Leach, J. M. *J. Inorg. Nucl. Chem.* **1972**, *34*, 885. (c) Bianchini, C.; Meli, A.; Nuzzi, F.; Dapporto, P. *J. Organomet. Chem.* **1982**, *236*, 245.

(17) The process has been theoretically analyzed by: Mealli, C., private communication. Some experimental evidence may be found in: Le Bozec, H.; Fillaut, J.-L.; Dixneuf, P. H. *J. Chem. Soc., Chem. Commun.* **1986**, 1182. Khasnis, D. V.; Le Bozec, H.; Dixneuf, P. H.; Adams, R. D. *Organometallics* **1986**, *5*, 1772. Bianchini, C.; Masi, D.; Meli, A.; Peruzzini, M.; Zanobini, F. *Organometallics* **1987**, *6*, 2557.

(18) Bianchini, C.; Meli, A. *J. Chem. Soc., Dalton Trans.* **1983**, 2419.

(19) (a) Hartzler, H. D. *J. Am. Chem. Soc.* **1973**, *95*, 4379. (b) Hartzler, H. D. *J. Am. Chem. Soc.* **1970**, *92*, 1412.

$C_{48}H_{55}ClI_3P_4RhS_2$: C, 43.05; H, 4.14; Rh, 7.68. Found: C, 43.12; H, 4.11; Rh, 7.59. The metathetical reaction of **5** with an equimolecular amount of $NaBPh_4$ in CH_2Cl_2–EtOH gave red-orange crystals of $[(triphos)RhCl(S_2CH(PEt_3))]BPh_4$ (**7**). When the latter reaction was carried out with a large excess of $NaBPh_4$, the compound $[(triphos)Rh(S_2CH(PEt_3))](BPh_4)_2$ (**6**) was obtained as red crystals in 85% yield. Anal. Calcd for $C_{96}H_{95}B_2P_4RhS_2$ (**6**): C, 73.85; H, 6.13; Rh, 6.59. Found: C, 73.74; H, 6.09; Rh, 6.51. Anal. Calcd for $C_{72}H_{75}BClP_4RhS_2$ (**7**): C, 67.69; H, 5.92; Rh, 8.05. Found: C, 67.50; H, 6.02; Rh, 7.99.

Reaction of 6 with (PPN)Cl. A DMF (10 mL) solution of (PPN)Cl (0.11 g, 0.2 mmol) and **6** (0.23 g, 0.15 mol) was stirred for 1 h. Compound **7** and $(PPN)BPh_4$ were isolated on addition of ethanol (70 mL).

Reaction of 1 with $NOBF_4$. A mixture of **1** (0.48 g, 0.5 mmol) and $NOBF_4$ (0.29 g, 1.5 mmol) in CH_2Cl_2 (30 mL) was stirred for 1 h. Within this time, a chromatic change from blue to red occurred. The unreacted excess of $NOBF_4$ was eliminated by filtration. On addition of ethanol (30 mL) and slow evaporation of the solvents, red-orange crystals of $[(triphos)RhCl(S_2CH(PEt_3))]BF_4$ (**8**) precipitated in 70% yield. They were filtered off and washed with ethanol and petroleum ether. Anal. Calcd for $C_{48}H_{55}BClF_4P_4RhS_2$: C, 55.16; H, 5.30; Rh, 9.85. Found: C, 54.99; H, 5.10; Rh, 9.60.

Reaction of 1 with $AgBF_4$. A 2-fold excess of $AgBF_4$ (0.19 g, 1 mmol) in THF (10 mL) was added to a stirred solution of **1** (0.48 g, 0.5 mmol) in THF (20 mL). The black precipitate of metallic silver, which separated during the reaction, was eliminated by filtration. Addition of ethanol (30 mL) to the resulting red solution led to the precipitation of **8** in 75% yield. When **1** was reacted with a 3-fold excess of $AgBF_4$, red crystals of $[(triphos)Rh(S_2CH(PEt_3))](BF_4)_2$ (**9**) were isolated in 80% yield. Anal. Calcd for $C_{48}H_{55}B_2F_8P_4RhS_2$: C, 52.58; H, 5.06; Rh, 9.38. Found: C, 52.47; H, 5.10; Rh, 9.25.

Reaction of 2 with I_2. I_2 (0.15 g, 0.6 mmol) was reacted with a solution of **2** (0.52 g, 0.5 mmol) in THF (30 mL). $NaBPh_4$ (0.68 g, 2 mmol) in ethanol (5 mL) was then added to the resulting red-brown solution and the mixture stirred for 1 h. On slow concentration, red-brown crystals of $[(triphos)Rh(Se_2CH(PEt_3))](BPh_4)_2$ (**10**) precipitated. They were filtered off and washed with ethanol and petroleum ether; yield 65%. Anal. Calcd for $C_{96}H_{95}B_2P_4RhSe_2$: C, 69.66; H, 5.79; Rh, 6.22. Found: C, 69.72; H, 5.80; Rh, 6.09. Compound **10** was obtained also by treating either a THF solution of **2** with $AgBF_4$ in THF or a CH_2Cl_2 solution of **2** with solid $NOBF_4$ and working up as above.

Reaction of 1 or 2 with HSO_3CF_3 (or $HBF_4{\cdot}OEt_2$). An equivalent amount of HSO_3CF_3 (or $HBF_4{\cdot}OEt_2$) was added to a solution of **1** or **2** (0.5 mmol) in THF (40 mL) containing $NaBPh_4$ (0.34 g, 1 mmol). An immediate reaction occurred as evidenced by a color change from blue (green for **2**) to red (red-brown for **2**). Crystals of **6** or **10** in 75% yield precipitated on standing for 1 h.

Reaction of 1 with $MeSO_3CF_3$. A mixture of **1** (0.48 g, 0.5 mmol), $MeSO_3CF_3$ (0.07 mL, 0.6 mmol), and $NaBPh_4$ (0.34 g, 1 mmol) was stirred for 1 h. Red crystals of $[(triphos)Rh(S_2CMe(PEt_3))](BPh_4)_2$ (**11**) were obtained from the resulting red solution in 80% yield on standing for 2 h. Anal. Calcd for $C_{97}H_{97}B_2P_4RhS_2$: C, 73.95; H, 6.21; Rh, 6.53. Found: C, 73.11; H, 6.26; Rh, 6.39.

Reaction of 5 or 7 with O_2. Dioxygen was bubbled through a DMF–CH_2Cl_2 (15 mL) solution of **5** or **7** (0.3 mmol) for 15 min. During this time the solution turned yellow and yellow crystals of $(triphos)RhCl(S_2CO)$ (**12**) precipitated on addition of a 3:1 mixture of ethanol and *n*-hexane (40 mL) and partial evaporation of the solvents.

Reaction of 6 and 11 with O_2. By workup as above red-brown crystals of $[(triphos)Rh(S_2CO)]BPh_4$ (**13**) were obtained.

Reaction of 10 with O_2. Greenish crystals of $[(triphos)Rh(Se_2CO)]BPh_4$ (**14**) were obtained by following the same procedure as above.

X-ray Data Collection and Reduction. Crystal data and data collection parameters are given in Table I. Intensity data were collected at room temperature (ca. 20 °C) on a Philips PW 1100 computer-controlled diffractometer equipped with a graphite monochromator. All the reflections with $6 < 2\theta < 50°$ were measured by the ω–2θ scan technique at a scan speed of 0.07°/s (in ω) with a variable scan width of (0.80 + 0.30 tan ω)° across the peak. Three standard reflections were measured every 120 min during data collection. No significant variation was noticed in their intensities. The standard deviations $\sigma(I)$ were estimated as previously reported[20] with an instability factor equal to 0.03. A reflection was considered unobserved when the net intensity I was $<3\sigma(I)$. An absorption correction, μ(Mo Kα) = 2.97 cm^{-1}, was applied by using the appropriate routines of the SHELX 76 system of programs (transmission factors varied between 0.88 and 0.93).[21] The intensity data were corrected for Lorentz and polarization effects. Atomic scattering factors were taken from ref 22 for non-hydrogen atoms and from ref 23 for hydrogen atoms. The anomalous dispersion correction was applied.[22]

Solution and Refinement of the Structure. The position of the rhodium atom was obtained from a Patterson synthesis. The positions of all of the other non-hydrogen atoms were obtained from successive Fourier maps. The structure was refined by full-matrix least squares using the SHELX 76 program. The function $\sum w(|F_o| - |F_c|)^2$ was minimized with weights $w = 1/\sigma^2(F_o)$. Phenyl groups were refined as rigid bodies with the assumption of D_{6h} symmetry for the rings. The hydrogen atoms were introduced in calculated positions (C–H distance of 1.08 Å) with an overall temperature factor U of 0.05 Å^2 and were not refined. Anisotropic temperature factors were used for Rh, S, and P atoms, whereas the other atoms were assigned isotropic thermal parameters. The final refinement gave an R value of 0.075, and R_w, defined as $[\sum w(|F_o| - |F_c|)^2/\sum w|F_o|^2]^{1/2}$, was 0.075. A final ΔF Fourier synthesis did not show remarkable features. The final values of the atomic parameters are reported in Tables III–V (Tables IV and V are supplementary material). A listing of F_o and F_c is available as supplementary material.

Registry No. **1**, 100044-10-8; **2**, 97689-96-8; **3**, 110416-97-2; **4**, 110391-67-8; **5**, 110391-69-0; **6**, 110391-71-4; **7**, 110391-72-5; **8**, 110391-73-6; **9**, 110391-74-7; **10**, 110391-76-9; **11**, 110391-78-1; **12**, 100044-11-9; **13**, 99955-64-3; **14**, 97689-99-1; I_2, 7553-56-2; EtOH, 64-17-5; $LiHBEt_3$, 22560-16-3; $HOSO_2CF_3$, 1493-13-6; $MeOSO_2CF_3$, 333-27-7; $NaBPH_4$, 143-66-8; O_2, 7782-44-7; $NOBPh_4$, 14635-75-7; $AgBF_4$, 14104-20-2; $[S_2CPEt_3]$, 3736-69-4; $[HS_2C(CH_3)PEt_3]$, 110375-42-3; $[HS_2CHPEt_3]$, 110375-43-4; $[Se_2CPEt_3]$, 110375-44-5; $[HSe_2CHPEt_3]$, 110375-45-6.

Supplementary Material Available: Positional parameters and isotropic temperature factors for the carbon atoms of the complex cation (Table IV) and for the atoms of the tetraphenylborate anions (Table V) (2 pages); a listing of observed and calculated structure factors (29 pages). Ordering information is given on any current masthead page.

(20) Corfield, P. W. R.; Doedens, R. J.; Ibers, J. A. *Inorg. Chem.* **1967**, *6*, 197.
(21) Sheldrick, G. M. "SHELX-76, Systems of Programs"; University of Cambridge: Cambridge, England, 1976.
(22) *International Tables for X-ray Crystallography*; Kynoch: Birmingham, England, 1974; Vol. IV.
(23) Stewart, R. F.; Davidson, E. R.; Simpson, W. T. *J. Chem. Phys.* **1965**, *42*, 3175.